Nonlinear Optics (WiSe 2017/18)
Lecture 22: January 16, 2018

12 High-harmonic generation and attoscience

12.1 Atomic units

12.2 The three-step model of HHG
12.2.1 Ionization
12.2.2 Propagation
12.2.3 Recombination

12.3 Attosecond pulses
12.3.1 The intensity challenge
12.3.2 The necessity of short driver pulses
12.3.3 Quantum diffusion
12.3.4 Propagation effects – phase matching
12.3.5 Optimizing HHG using cycle-sculpted driver waveforms

Electromagnetic spectrum from IR to hard X-rays

electronic dynamics

electronic+structural dynamics

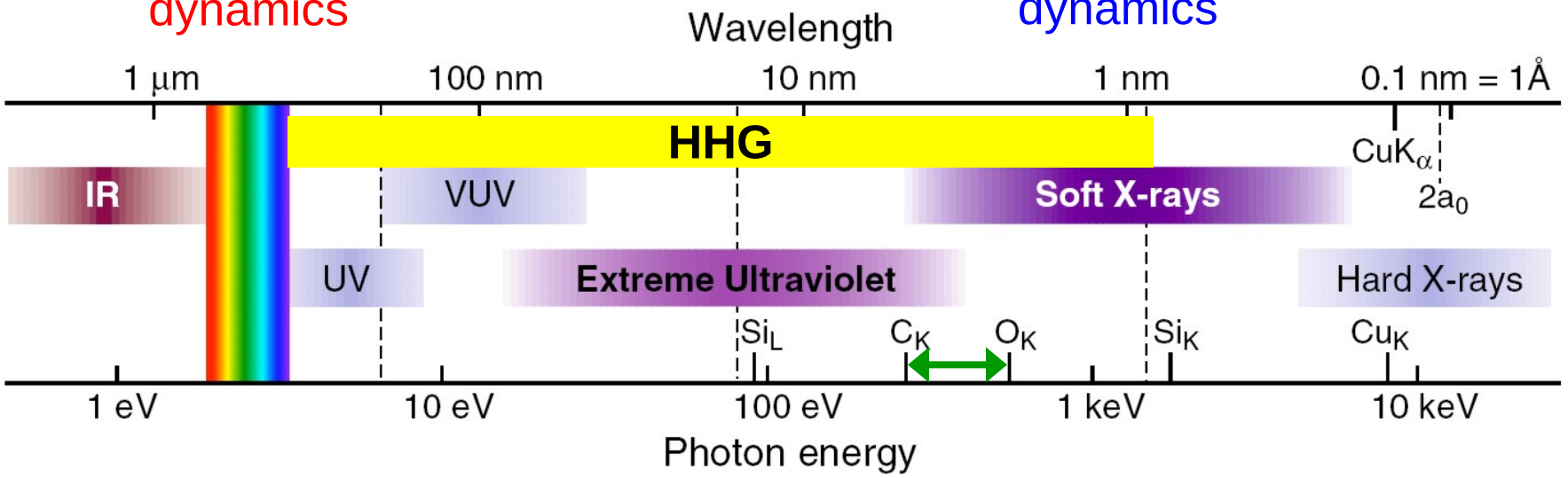

$2a_0$=1.06 Å (n=1 orbit in hydrogen)

"water window"

C_K @ 284 eV or 4.37 nm

O_K @ 543 eV or 2.28 nm

D. Attwood and A. Sakdinawat, *Soft X-Rays and Extreme Ultraviolet Radiation* (2nd edition, Cambridge, 2016)

12. High-harmonic generation and attoscience

HHG: The three step model

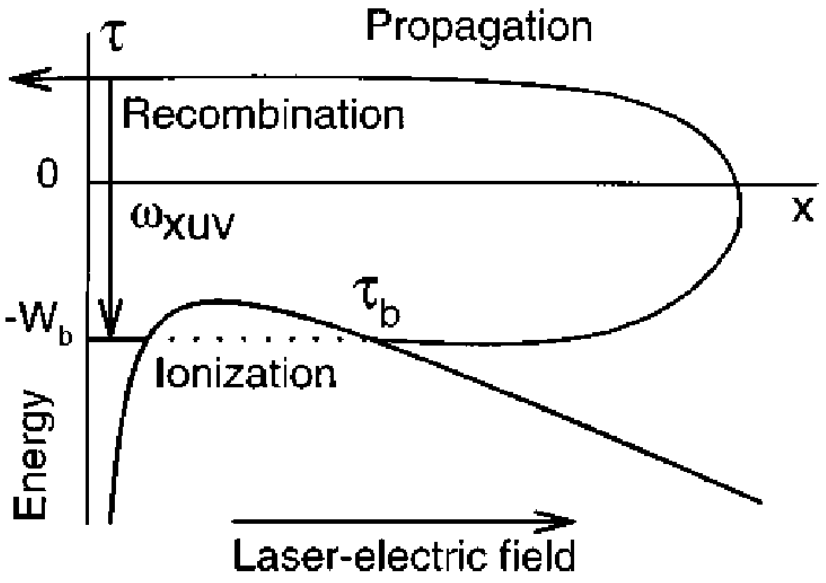

12.1 Atomic units

Hydrogen Atom

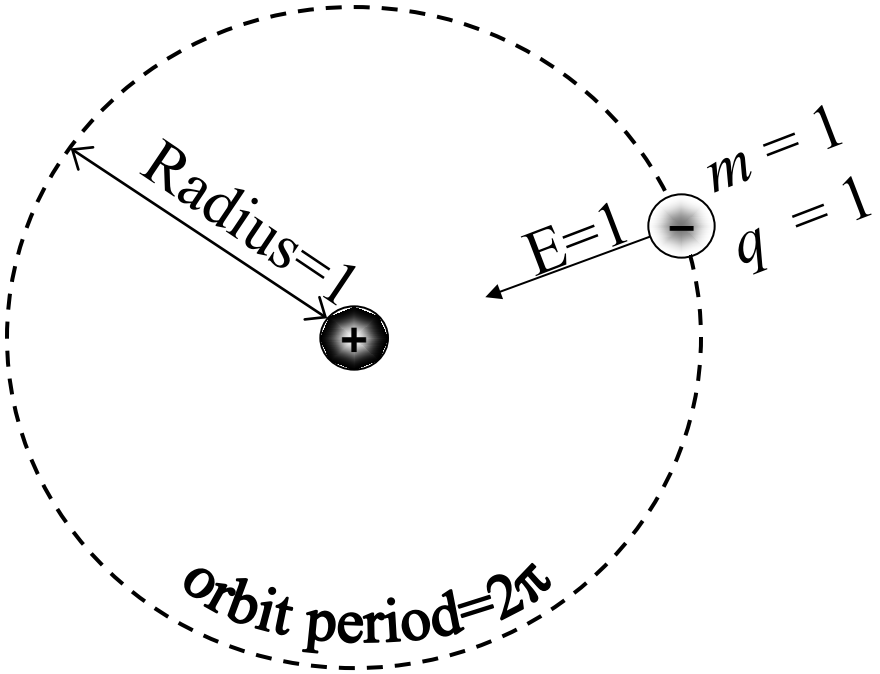

P. B. Corkum, PRL **71**, 1994 (1993)
K. J. Schafer, B. Yang, L. DiMauro,
and K. C. Kulander, PRL **70**, 1599 (1993)
M. Y. Kuchiev, JETP Lett. **45**, 404 (1987)

and

$\hbar = 1$

Atomic unit of...	Definition	In SI units
Electric charge	The electron charge	1.602×10^{-19} C
Mass	The electron mass	9.109×10^{-31}kg
Length	The Bohr radius	5.2917×10^{-11}m
Time	$1/2\pi$ of the first Bohr orbit period	24.189 asec
Energy	The potential energy of the electron in the first Bohr orbit	27.21eV= $= 4.359 \times 10^{-18} J$
Electric field	The electric field at the first Bohr orbit	5.142×10^{11}V/m = E_a

perturbative nonlinear optics:

$$P = \epsilon_0 \left(\chi^{(1)} E + \chi^{(2)} E^2 + \chi^{(3)} E^3 + ...\right)$$

E-field in units of E_a: susceptibilities of order 1

$\chi^{(n)} = \chi^{(n-1)}/E_a$ $\chi^{(2)} \sim 10^{-12}/(V/m)$ $\chi^{(3)} \sim 10^{-23}/(V/m)^2$

A typical field amplitude for HHG in helium is 0.3 au $\approx 1.7 \times 10^9$V/cm. The corresponding intensity is $0.5 \cdot E^2/377\Omega \approx 4 \times 10^{15}$W/cm^2. For a Ti:sapphire beam (800 nm wavelength) focused to a 25μm^2 spot and for a pulse duration of 10 fs we find that the pulses should carry about 0.1 mJ of energy.

12.2 The three-step model of HHG

12.2.1 First step - ionization

multiphoton ionization

$$\omega < I_p \ (\hbar\omega < I_p)$$

Keldysh parameter:

$$\gamma = \omega\sqrt{2I_p}\Big/E > 1$$

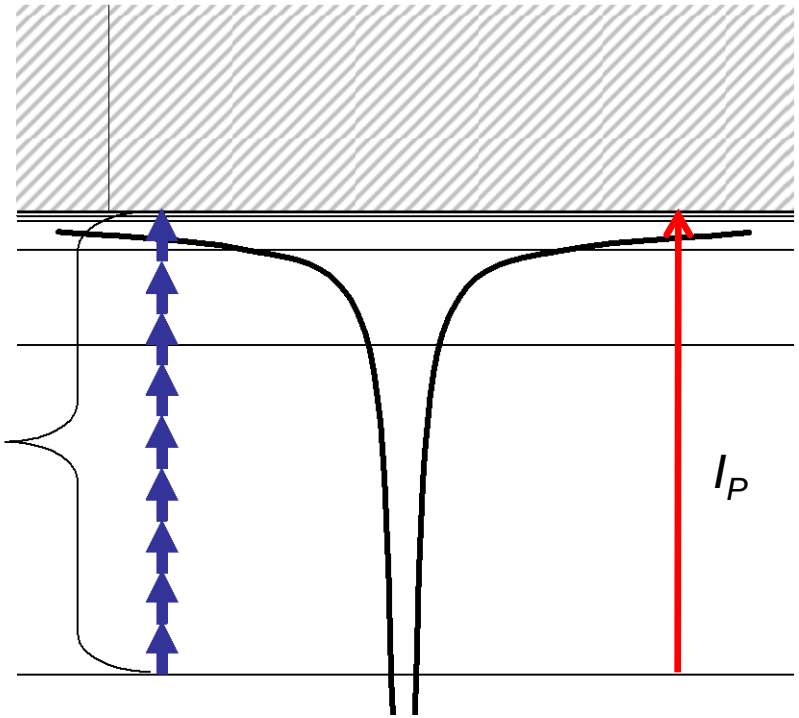

tunneling regime

barrier-suppression regime

dominant when: $U_p \gtrsim I_p$

ponderomotive energy:

$$U_p = \left(\frac{qE}{2m\omega}\right)^2 = \left(\frac{E}{2\omega}\right)^2$$

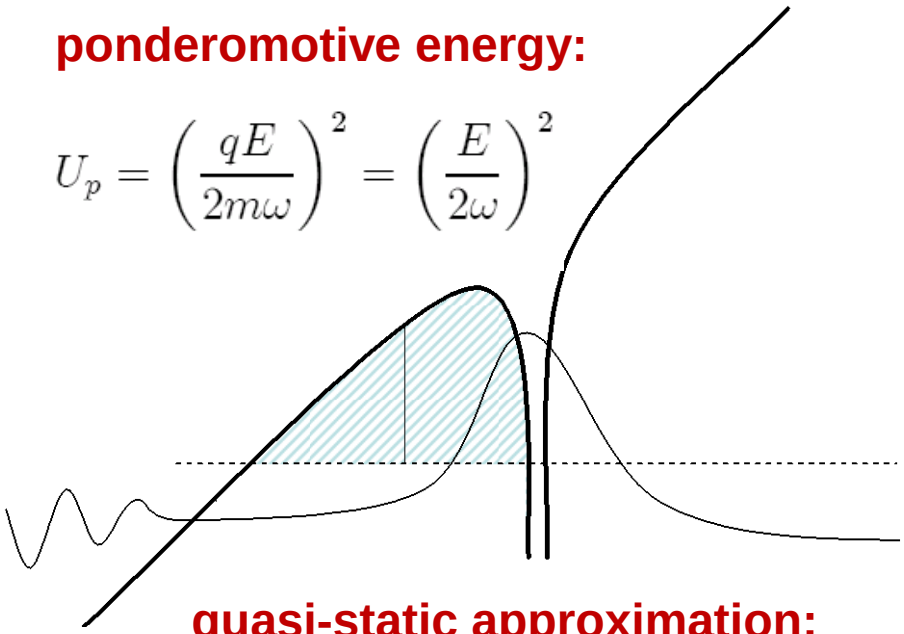

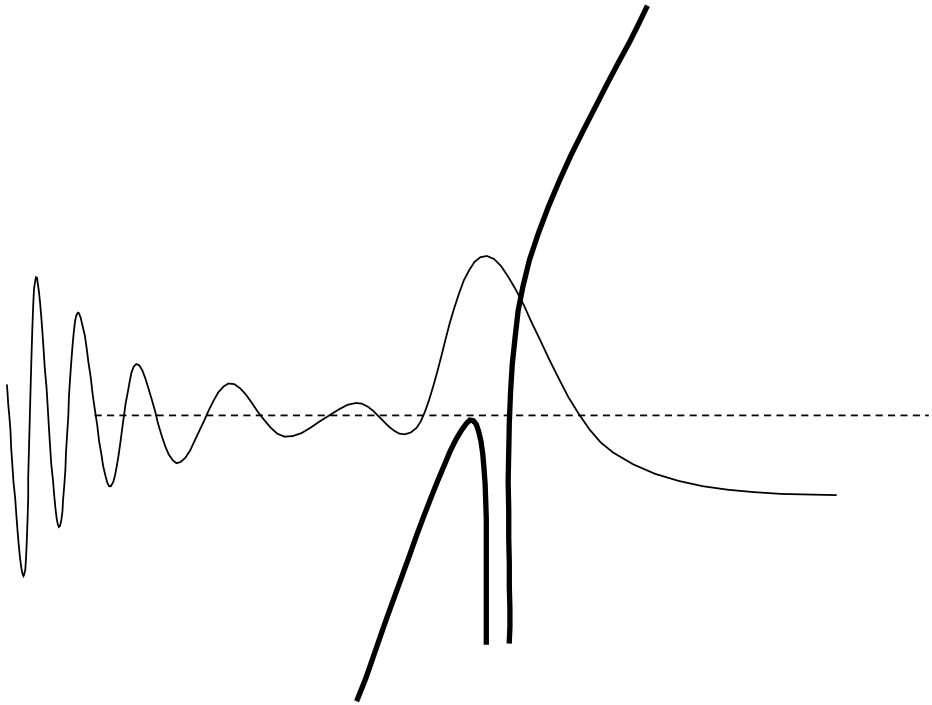

quasi-static approximation:

$$w(E) \sim \exp\left(-\frac{2(2I_p)^{3/2}}{3E}\right)$$

emission probability linear in field

$$|a(t)|^2 = \exp\left(-\int_0^t w(E(t'))dt'\right)$$

ionization rates

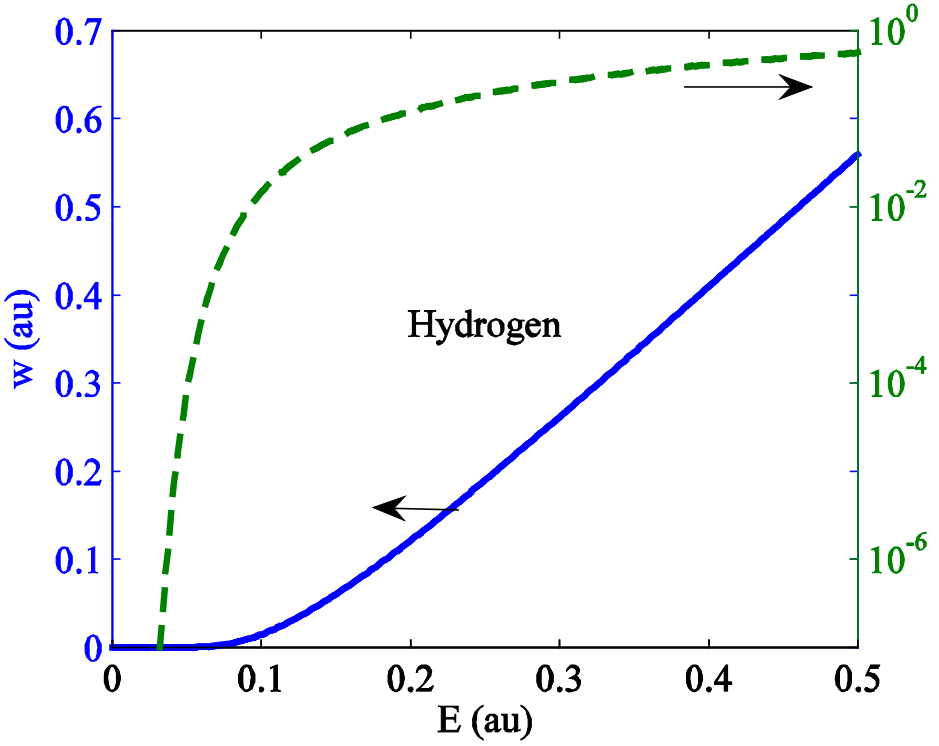

Figure 12.6: Static ionization rate for hydrogen on a linear and logarithmic scale

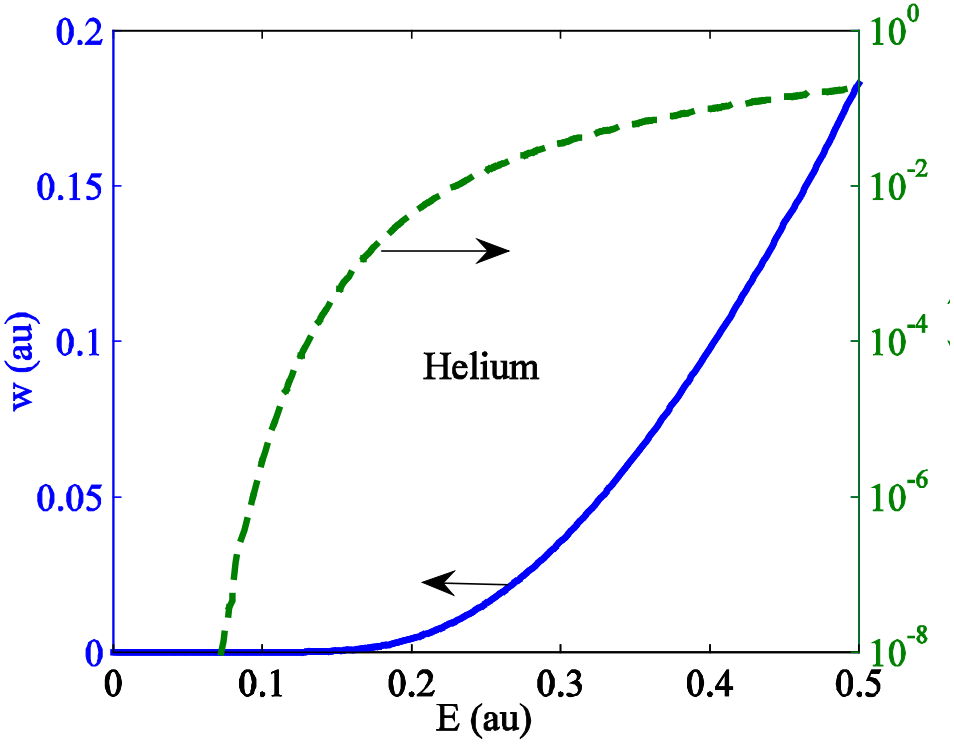

Figure 12.7: Static ionization rate for helium on a linear and logarithmic scale

12.2.2 Propagation

$$\ddot{x}(t) = E_0 \cos \omega t$$

$$\dot{x}(t) = \frac{E_0}{\omega} \sin \omega t - \frac{E_0}{\omega} \sin \omega t_0$$

$$x(t) = -\frac{E_0}{\omega^2} \cos \omega t - (t - t_0)\frac{E_0}{\omega} \sin \omega t_0 + \frac{E_0}{\omega^2} \cos \omega t_0,$$

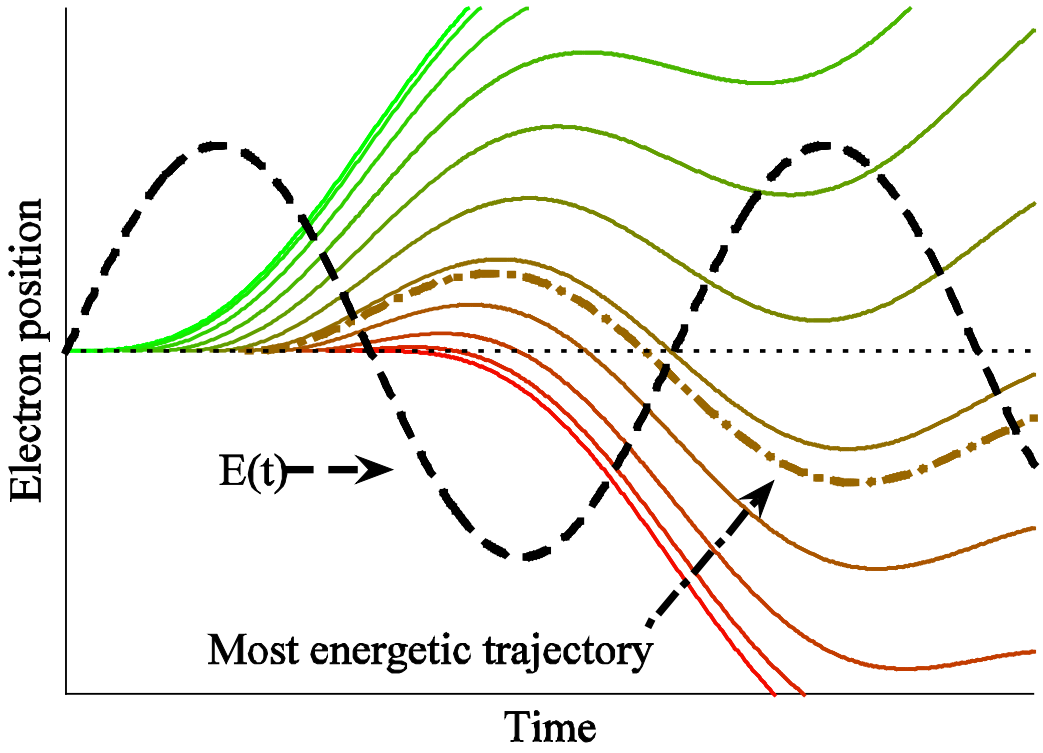

Figure 12.8: Electron trajectories

Trajectory with maximum kinetic energy

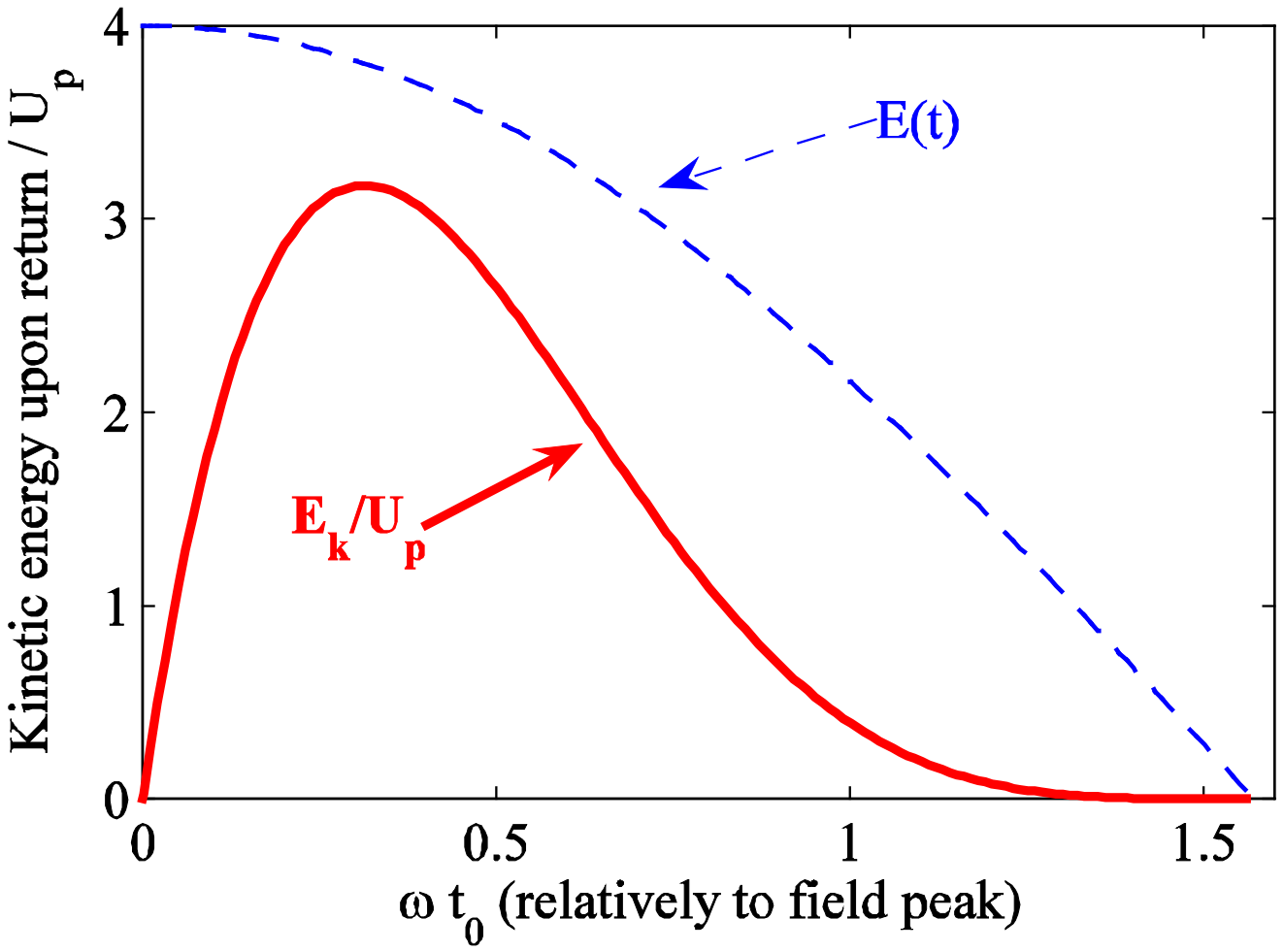

maximum for $\omega t \approx 0.31$ $E_k = 3.17 U_p$ $U_p = \frac{1}{2}\left(\frac{E}{\omega}\right)^2$

12.2.3 Recombination

Schrödinger equation in dipole approximation

$$i\frac{d}{dt}\left|\psi\right\rangle = H\left|\psi\right\rangle - E(t)x$$

atomic Hamiltonian

$$H = -\frac{1}{2}\nabla + V(\vec{r}),$$

wavefunction of partially ionized atom

$$\left|\psi(t)\right\rangle = a(t)\left|0\right\rangle + \left|\varphi(t)\right\rangle$$

dipole moment

$$\vec{d}(t) = \left\langle\psi(t)\right|\vec{x}\left|\psi(t)\right\rangle$$

dipole acceleration and Ehrenfest theorem

$$\ddot{\vec{x}} = -\nabla V(\vec{r}) + E(t)$$

$$\begin{aligned}
\ddot{\vec{d}}_{HHG}(t) &= -\langle\psi(t)|\nabla V(\vec{r})|\psi(t)\rangle \\
&= -|a(t)|^2\langle 0|\nabla V(\vec{r})|0\rangle - a(t)\langle\varphi(t)|\nabla V(\vec{r})|0\rangle \\
&\quad -a^*(t)\langle\psi(t)|\nabla V(\vec{r})|0\rangle - \langle\varphi(t)|\nabla V(\vec{r})|\varphi(t)\rangle . \\
&\tilde{} -a^*(t)\langle\varphi(t)|\nabla V(\vec{r})|0\rangle - a(t)\langle 0|\nabla V(\vec{r})|\varphi(t)\rangle \\
&= \ddot{\xi}(t) + \ddot{\xi}^*(t), \text{ with } \ddot{\xi}(t) = -a^*(t)\langle\varphi(t)|\nabla V(\vec{r})|0\rangle
\end{aligned}$$

after some calculations

$$\ddot{\xi}(t) = 2^{3/2}\pi(2I_P)^{1/4}e^{i\pi/4}\sum_n \frac{a(t_{nb}(t)a(t)\sqrt{w(Et_{nb}(t))}}{E(t_{nb}(t))(t-t_{nb}(t))^{3/2}}\vec{\alpha}_{rec}e^{-iS_n(t)}$$

Lewenstein model: Strong-Field Approximation (SFA)

Vladimir P. Krainov: “But the Schrödinger equation is useless!”

$$\vec{d}[\vec{k}] = \left\langle \vec{k} \middle| \vec{r} \middle| 0 \right\rangle$$

$$P_z = 2\,\mathrm{Re} \int d^3\vec{k} \int_{-\infty}^{t} dt' \underbrace{e^{iE_0 t} d_z^*\left[\vec{k} - \vec{A}(t)\right]}_{\text{recombination}} \underbrace{e^{\frac{i}{2}\int_{t'}^{t} d\tau [\vec{k} - \vec{A}(\tau)]^2}}_{\text{propagation}} \underbrace{e^{-iE_0 t'} E_z(t') d_z\left[\vec{k} - \vec{A}(t')\right]}_{\text{ionization}}$$

Volkov phase

M. Lewenstein *et al.,* PRA **49**, 2117 (1994)

Improved Lewenstein model

$$\frac{d^2}{dt^2}\langle x\rangle = \frac{1}{\sqrt{\pi}}\left(2I_p\right)^{\frac{1}{4}} e^{\frac{3i\pi}{4}} a(t)\times \sqrt{\frac{I_p}{\pi}}\exp\left(-\frac{\left(2I_p\right)^{\frac{3}{2}}}{3|E|}\right)$$

$$\sum_n \frac{\sqrt{w\left(E\left[t_{bn}(t)\right]\right)}\,\mathcal{I}\left[t_{bn}(t)\right]}{E\left[t_{bn}(t)\right]} \times \frac{(2\pi)^{\frac{3}{2}} e^{-iS_n(t)}}{\left[t-t_{bn}(t)\right]^{\frac{3}{2}}} \times \left\langle 0\left|\partial_x V(\mathbf{r})\right|\mathrm{v}_x\right\rangle + c.c.$$

ionization — propagation — recombination

$t_{bn}(t)$ – birth time of trajectory n recolliding at time t

$w(E)$ – static ionization rate, $e^{-iS_n(t)}$ - stationary action

M. Y. Ivanov, T. Brabec, and N. Burnett, PRA **54**, 742 (1996)

A. Gordon and F. X. Kärtner, PRL **95**, 223901 (2005)

V. M. Gkortsas *et al.*, J. Phys. B **44**, 045601 (2011)

12.2.3 Recombination

$$\omega_{\mathrm{hmax}} = I_p + 3.17U_p$$

Ideal sinusoidal single-cycle pulse $E(t) = E_0 \sin \omega t$.

secant hyperbolic pulse with 5-fs FWHM duration and a max. field amplitude of 0.12 au

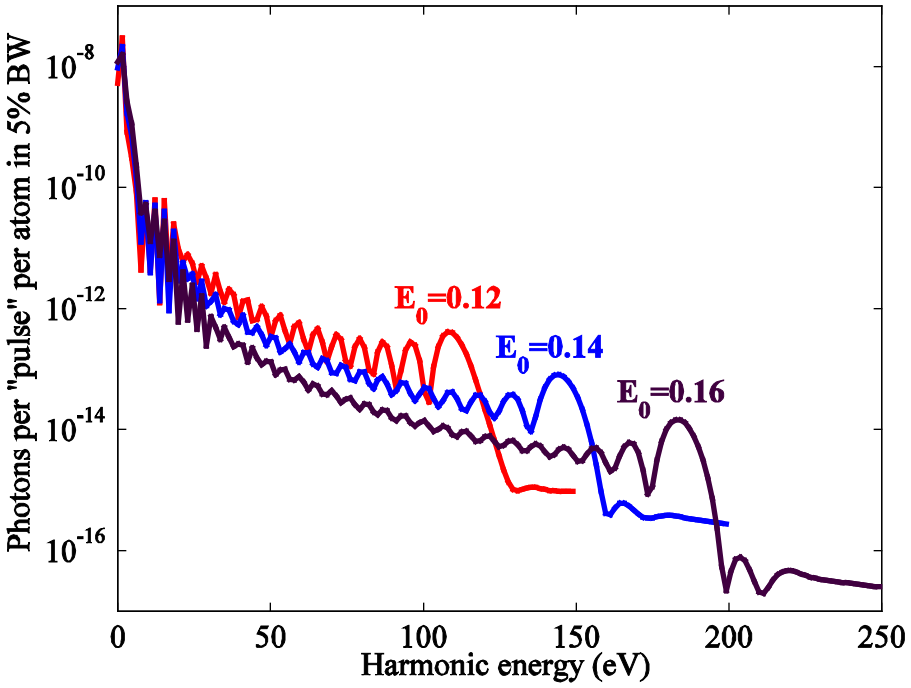

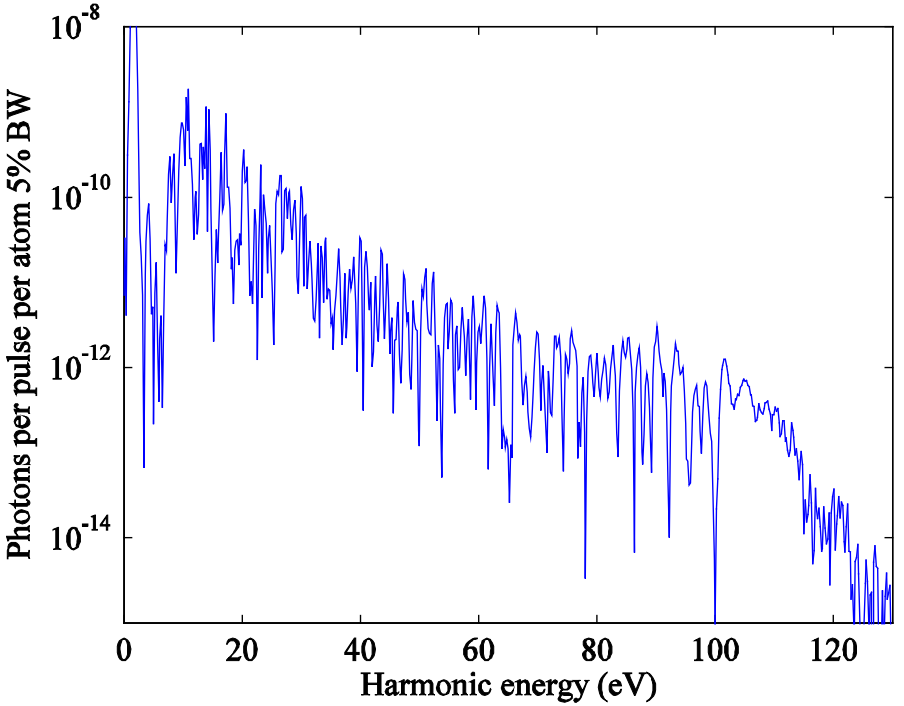

Figure 12.10-13: Simulated HHG spectra for hydrogen excited by Ti:sapphire pulses (800 nm, corresponding to ω = 0.057au)

Long and short trajectories

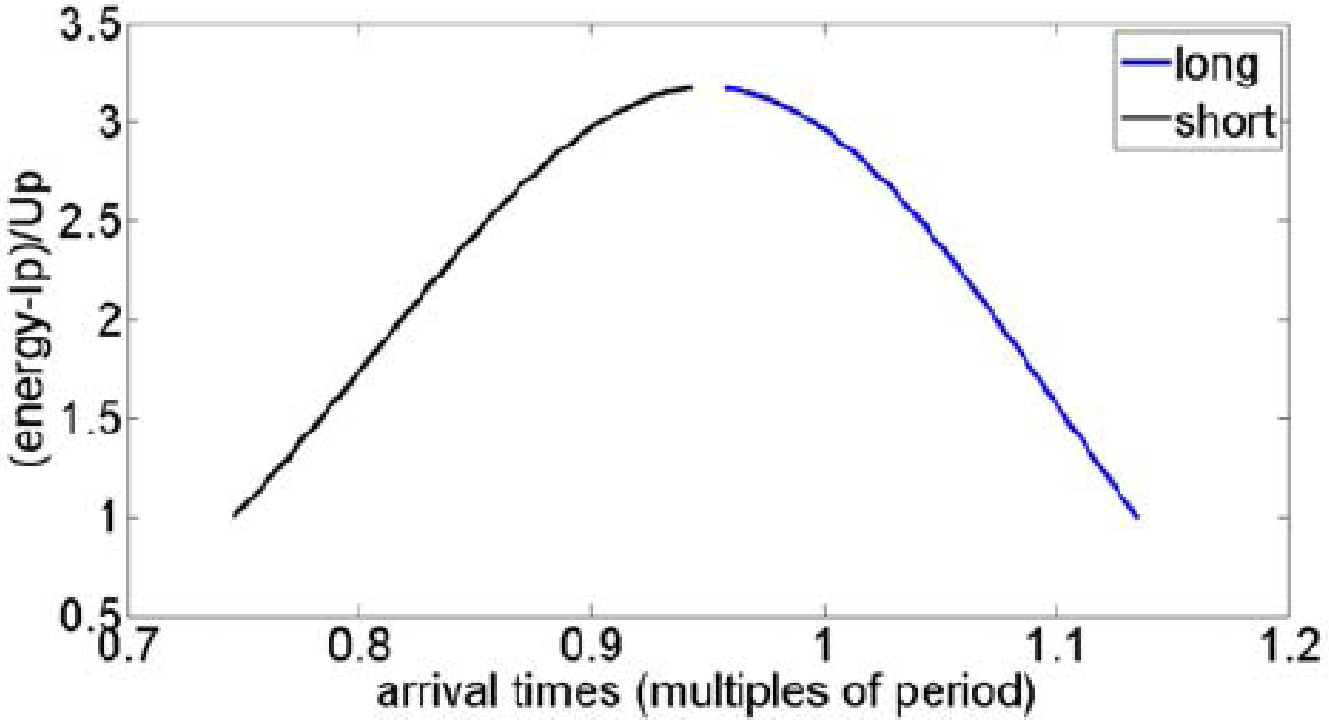

Figure 12.11: Kinetic energy of long and short trajectories

12.3 HHG from multi-cycle fields

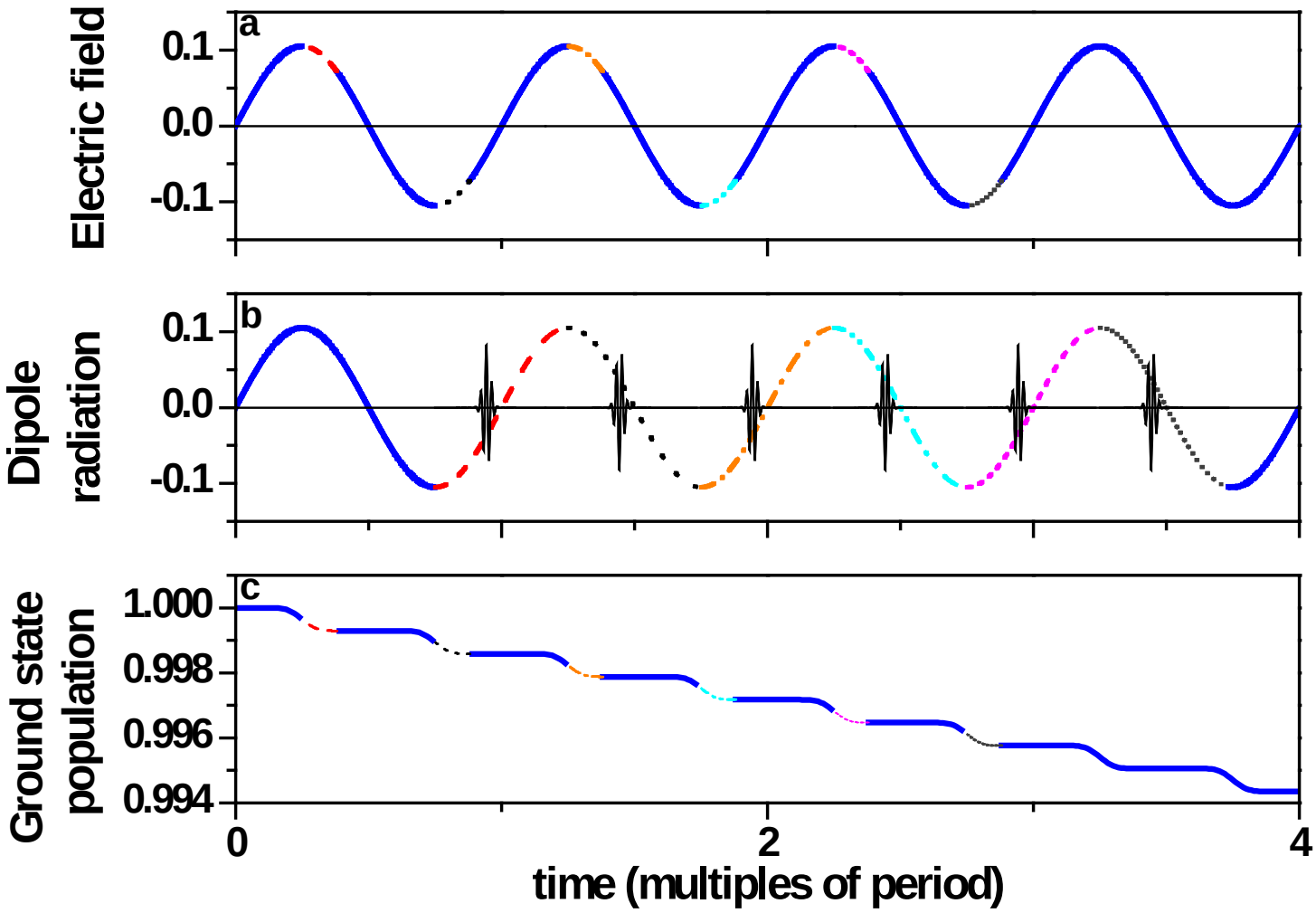

HHG experiment and theory

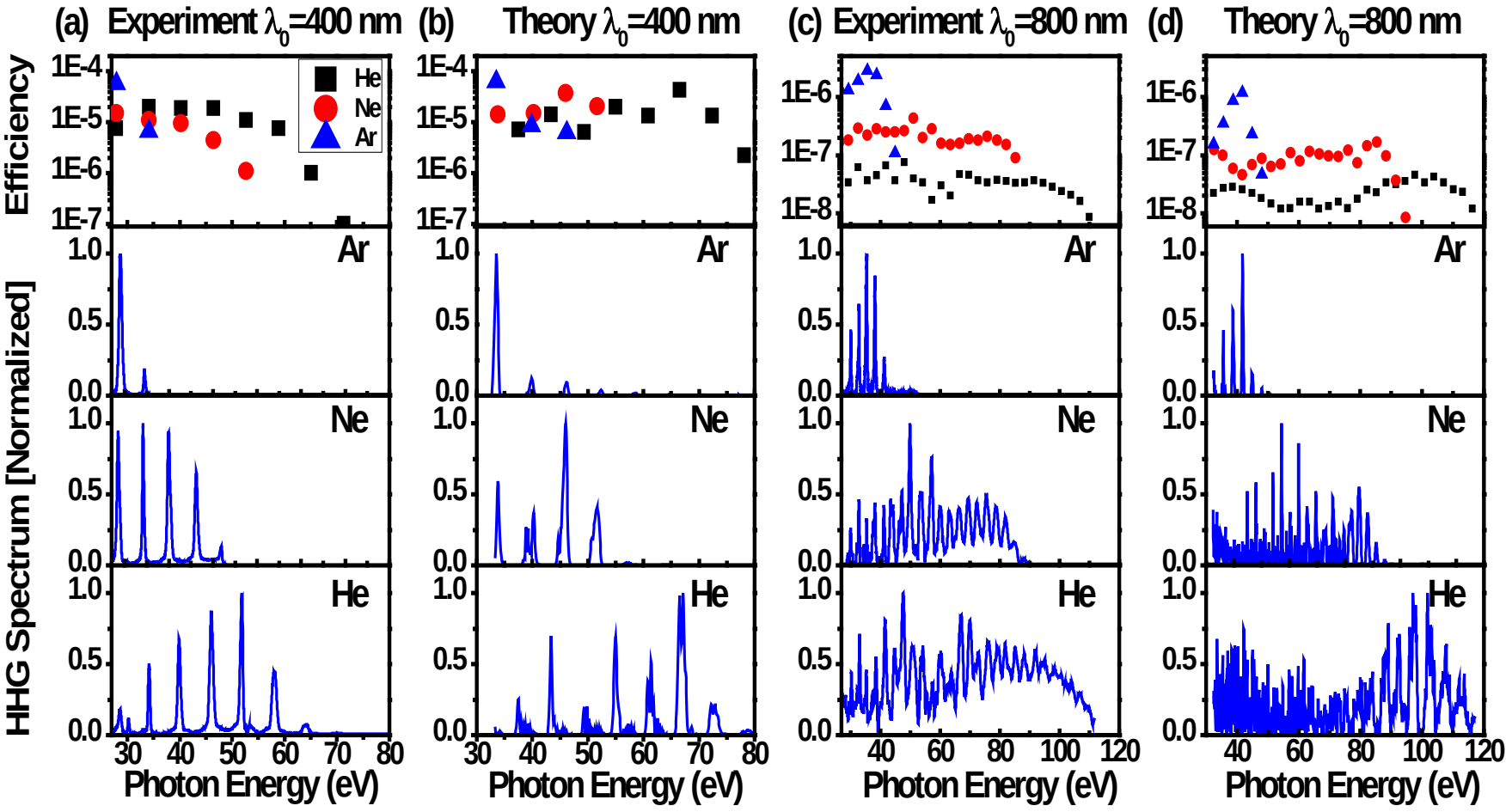

a) Experimental results for HHG driven by 400 nm, 1 mJ and 26 fs driver pulses with beam waist 30 μm: top row, efficiencies for Ar (50 mbar), Ne (300 mbar) and He (2 bar) using a 2 mm long nozzle; remaining rows, the respective normalized HHG spectra. b) Simulation results for Ar (2.5×10^{14} W/cm^2), Ne (5.3×10^{14} W/cm^2) and He (8.5×10^{14} W/cm^2) for the same interaction parameters like in (a). c) Experimental results for HHG driven by 800 nm, 35 fs driver pulses with beam waist 40 μm: top row, efficiencies for Ar (50 mbar, 0.6 mJ), Ne (300 mbar, 2 mJ) and He (2 bar, 2 mJ) using a 2 mm long nozzle; remaining rows, the respective normalized HHG spectra. d) Simulation results for Ar (1.2×10^{14} W/cm^2), Ne (3.2×10^{14} W/cm^2) and He (7.4×10^{14} W/cm^2) for the same interaction parameters like in (c)

12.3 Attosecond pulses

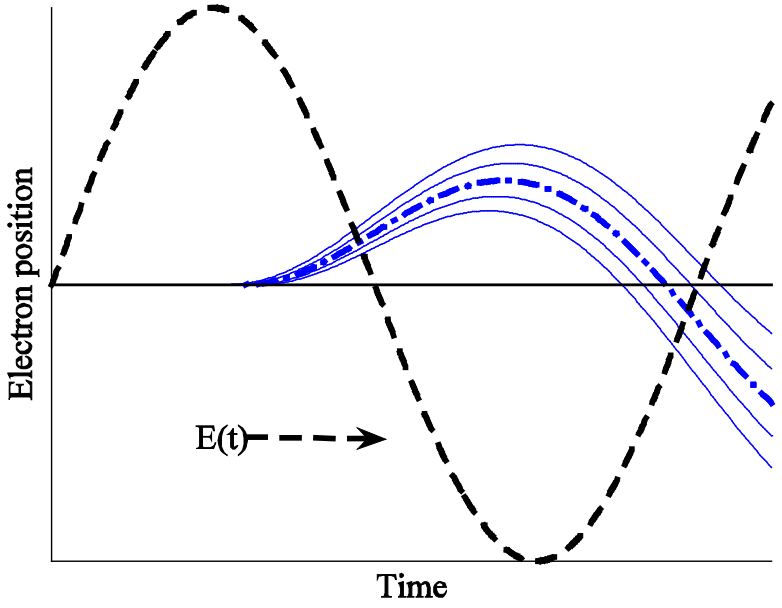

Figure 12.14: Neighborhood of the most energetic trajectory, which is responsible for the highest-frequency radiation (cutoff) emitted

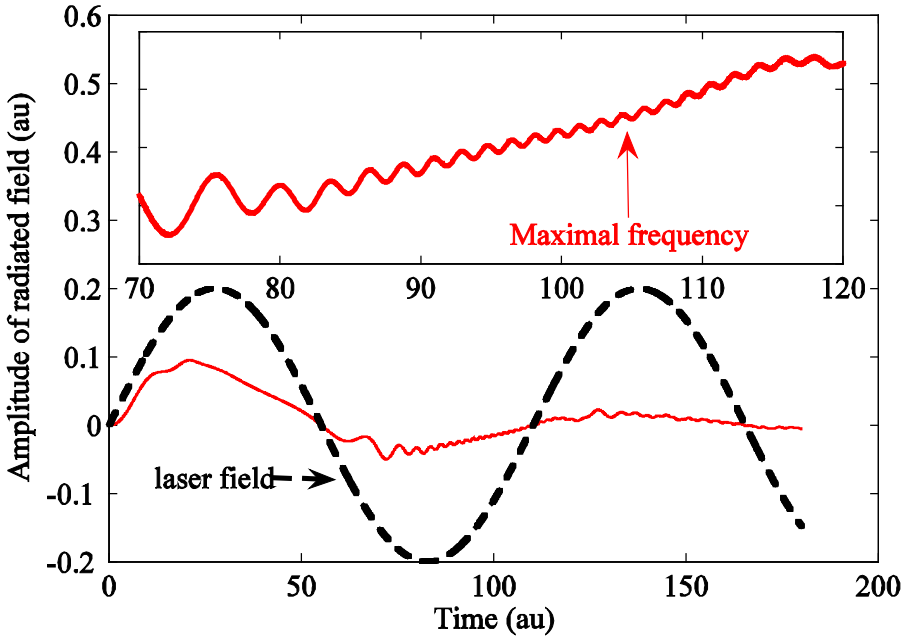

Figure 12.15: (a) Amplitude of radiated HHG field for the same parameters as Fig. 13.9. Note the chirp

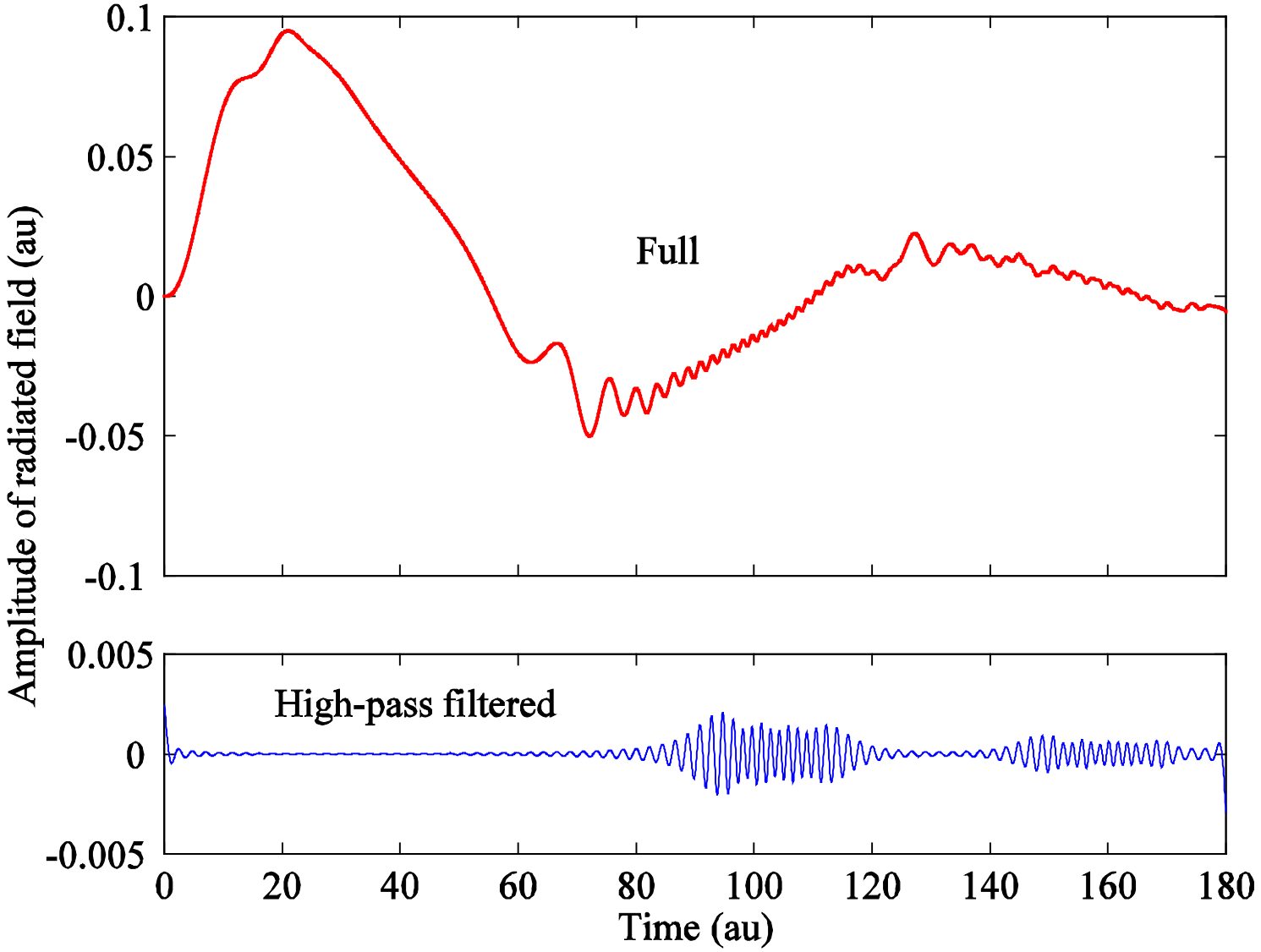

Figure 12.16: The same as Fig. 13.11a, before and after high-pass filtering

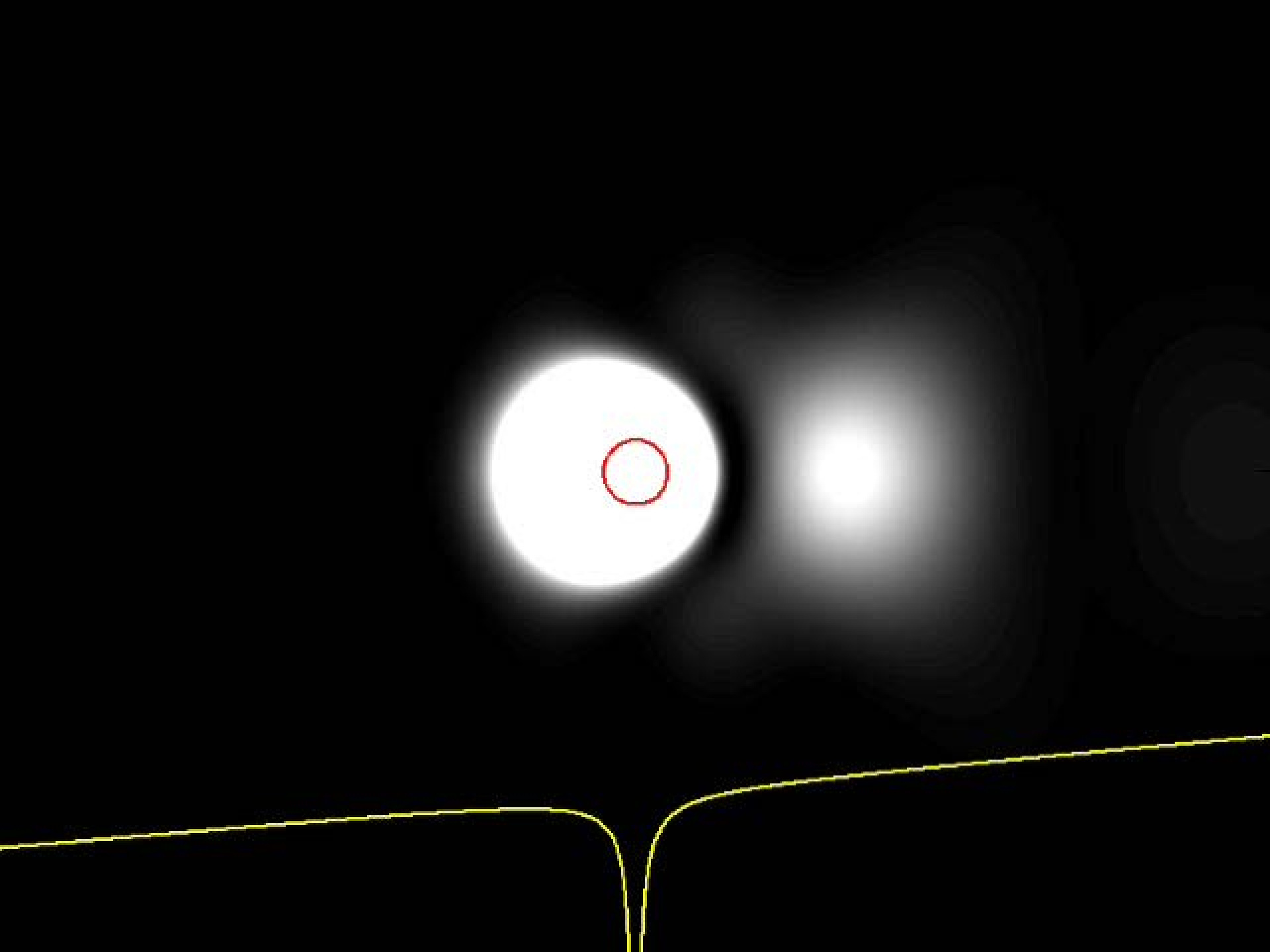

Figure 13.17: Ionization of helium in the presence of a linearly polarized electric field of a laser pulse with 800nm wave-length and a peak intensity $4 \times 10^{15} W/cm^2$:
(a) electric field;
(b) fraction of ionized electrons;
(c) instantaneous ionization rate
The thin and thick lines represent pulses of durations of 50 fs and 5 fs FWHM, respectively

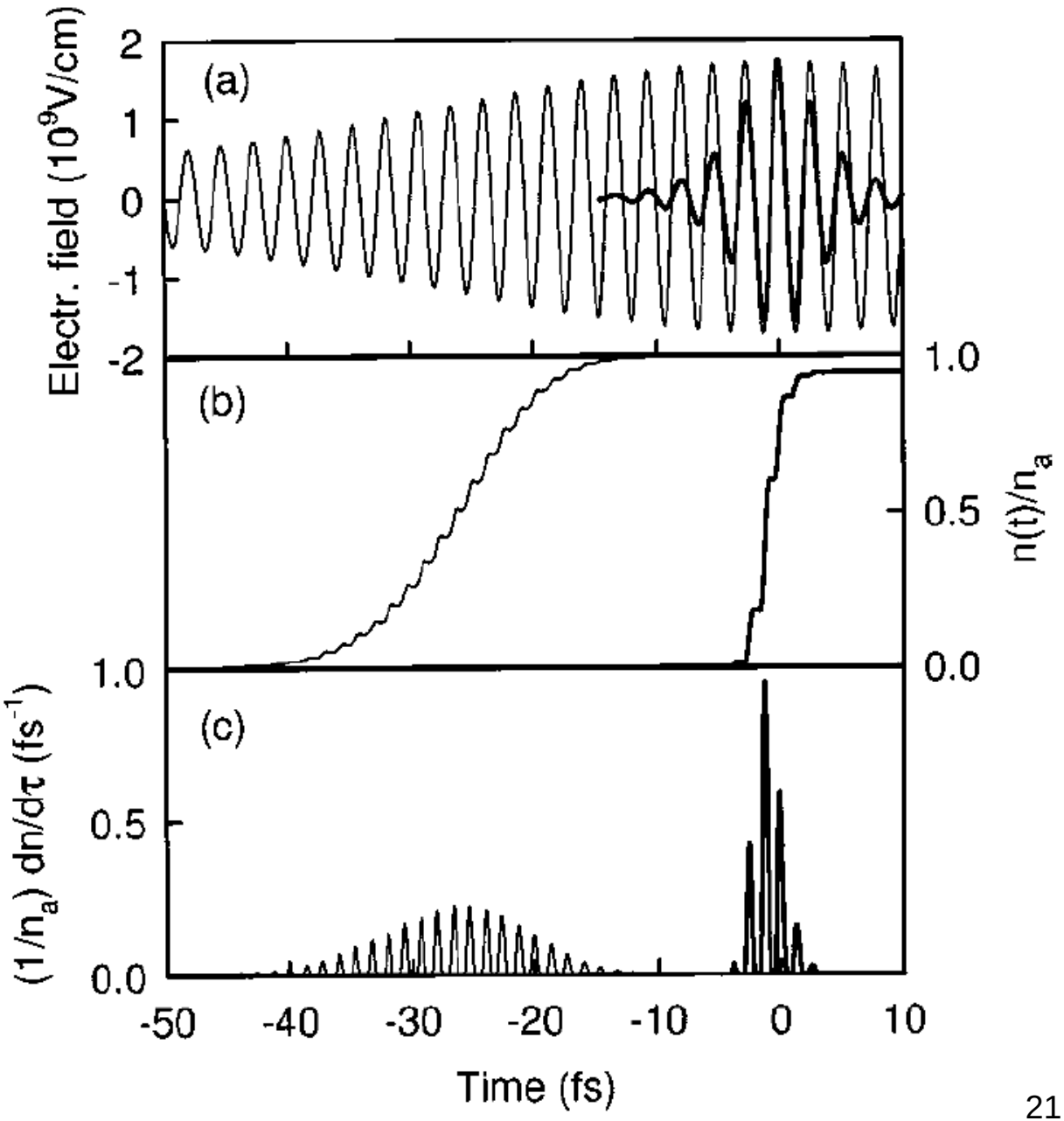

other difficulties:

quantum diffusion

phase matching

12.3.3 Quantum diffusion and λ-scaling laws

- Keldysh parameter $\sim\lambda^{-1}$ → tunneling regime for IR driver pulses
- electron energies $\sim\lambda^{2}$ → laser-induced electron diffraction
- HHG cutoff $\sim\lambda^{2}$ → keV HHG photons
- minimum attosecond pulse duration $\sim\lambda^{-1/2}$ → shorter X-ray pulses
- HHG efficiency $\sim\lambda^{-(5\text{-}6)}$

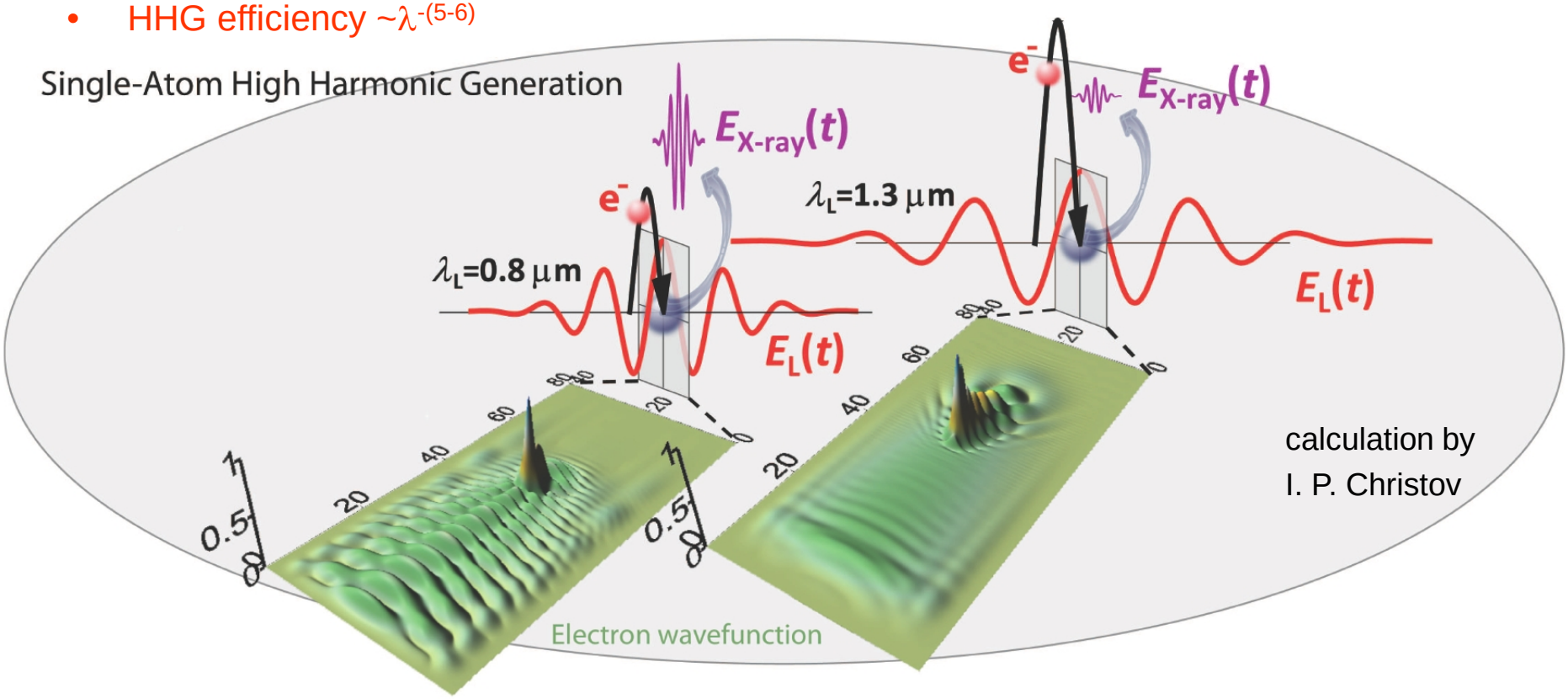

B. Sheehy *et al.*, PRL **83**, 5270 (1999)
B. Shan et al., PRA **65**, 011804(R) (2001)
A. Gordon *et al.*, Opt. Express **13**, 2941 (2005)
J. Tate *et al.*, PRL **98**, 013901 (2007)
K. Schiessl *et al.*, PRL **99**, 253903 (2007)

P. Colosimo *et al.*, Nature Physics **4**, 386 (2008)
G. Doumy *et al.*, PRL **102**, 093002 (2009)
C. I. Blaga *et al.*, Nature Physics **5**, 335 (2009)
A. D. Shiner *et al.*, PRL **103**, 073902 (2009)
C. Vozzi *et al.*, PRA **79**, 033842 (2009)

12.3.4 Macroscopic aspects of phase-matched HHG

tight focusing geometry **plane-wave propagation**

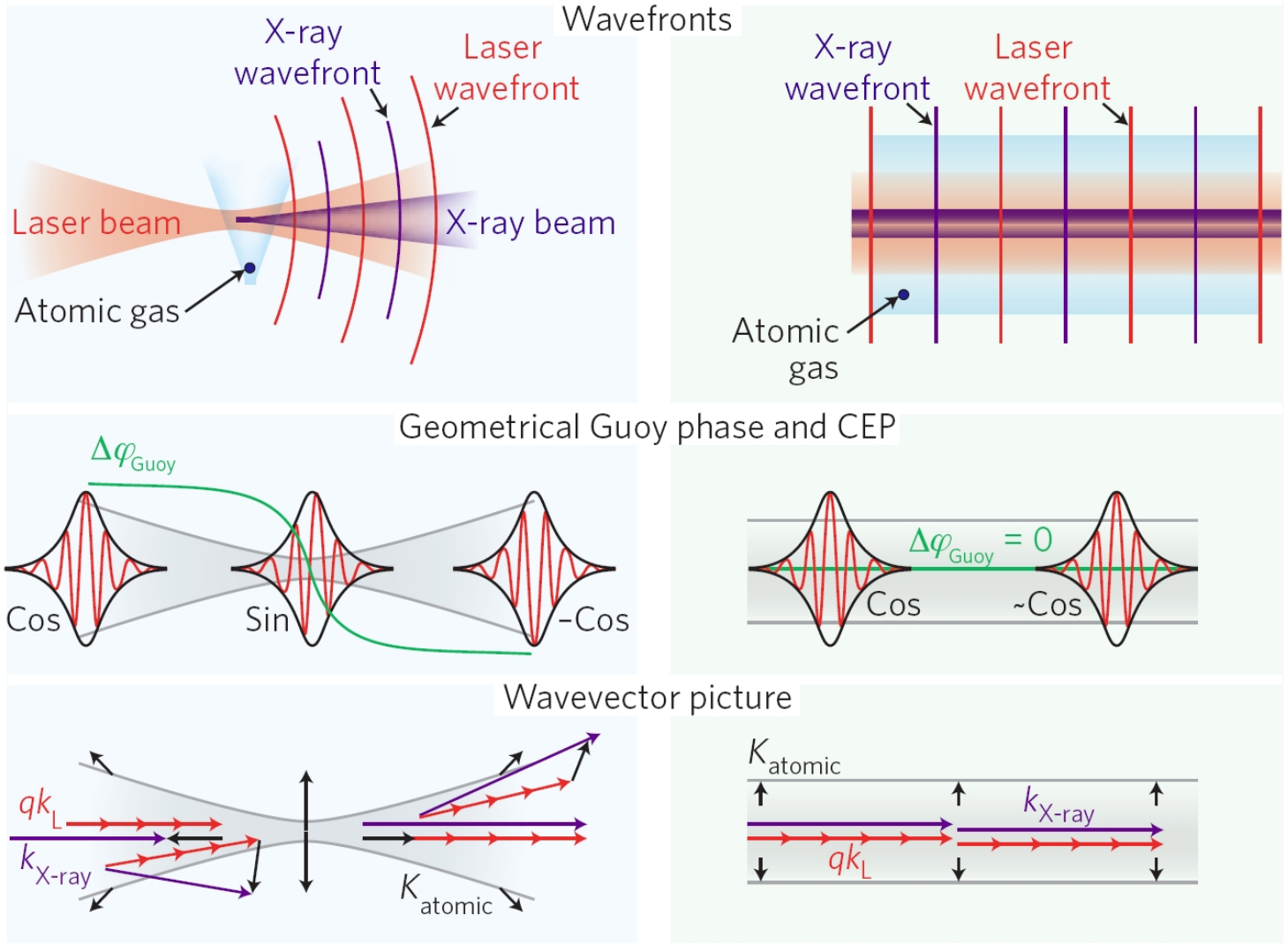

T. Popmintchev *et al.*, Nature Photonics **4**, 822 (2010)

Phase-matched HHG with mid-IR pulses

u_{11} mode factor

p pressure in atm

η ionization fraction

$\tilde{n}_2$ nonlinear refractive index coeff. per atm

N_a number density of atoms per atm

$$\Delta k \approx \underbrace{q\frac{u_{11}^2\lambda_L}{4\pi a^2}}_{\text{waveguide}} - \underbrace{qp(1-\eta)\frac{2\pi}{\lambda_L}(\Delta\delta + \tilde{n}_2 I)}_{\text{neutral atoms}} + \underbrace{qp\eta N_a r_e \lambda_L}_{\text{free electrons}}$$

0 for loose-focusing geometry

q harmonic order

a inner wave-guide radius

$\Delta\delta = n_{gas}(\lambda_L) - n_{gas}(\lambda_L/q)$ at 1atm

r_e classical electron radius

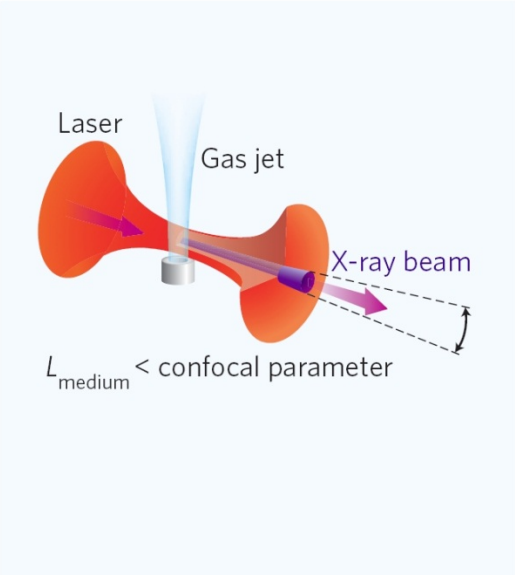

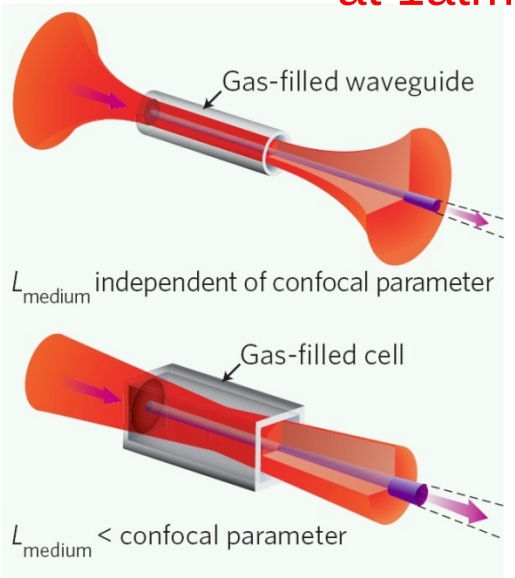

T. Popmintchev *et al.*,
PNAS **106**, 10516 (2009)
Nature Photonics **4**, 822 (2010)

E. J. Takahashi *et al.*,
PRL **101**, 253901 (2008)
PRA **66**, 021802 (2002)
IEEE JSTQE **10**, 1315 (2004)

Phase-matched HHG versus driver wavelength

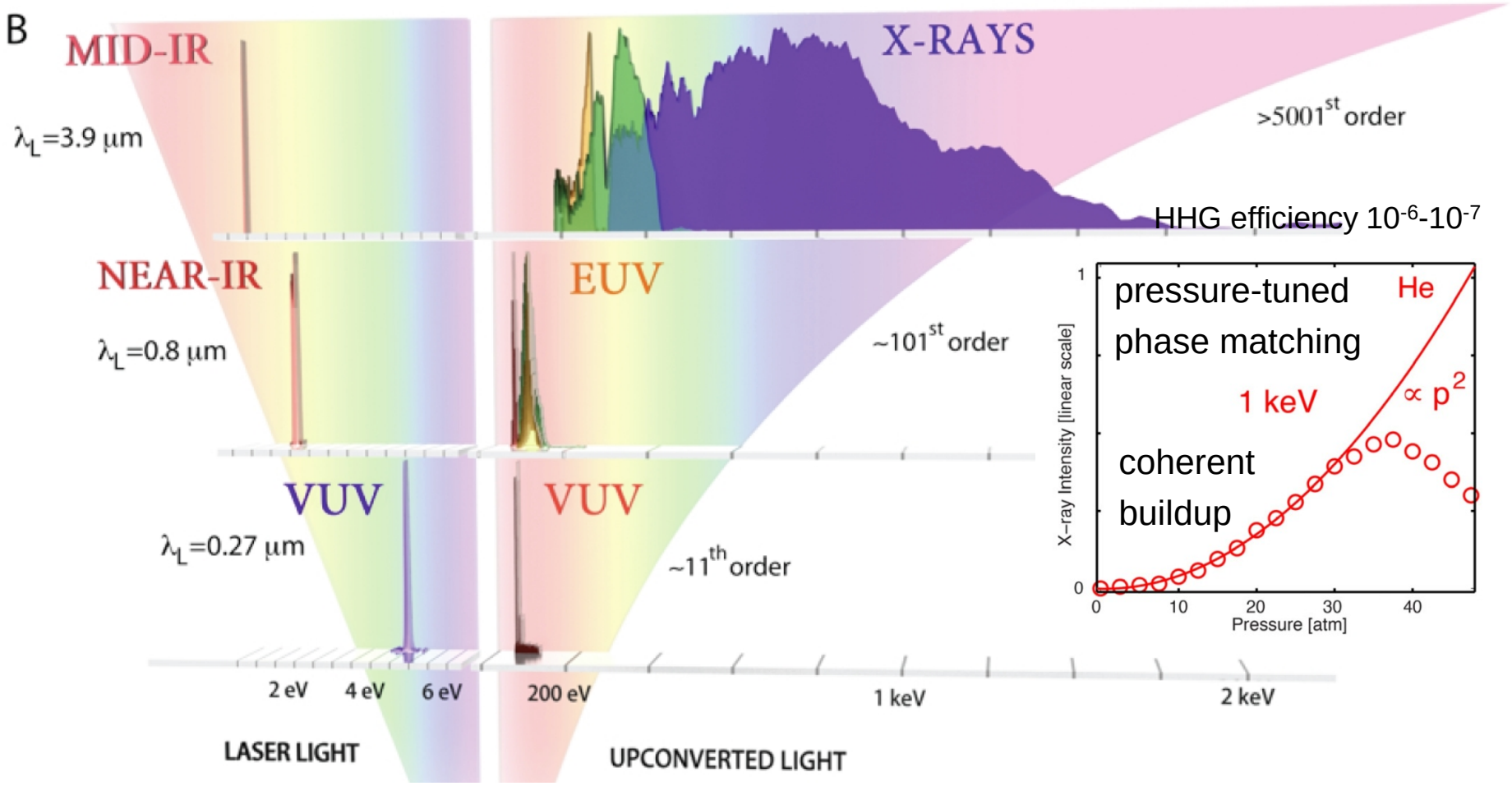

T. Popmintchev *et al.*, Science **336**, 1287 (2012)

HHG phase-matching cutoffs

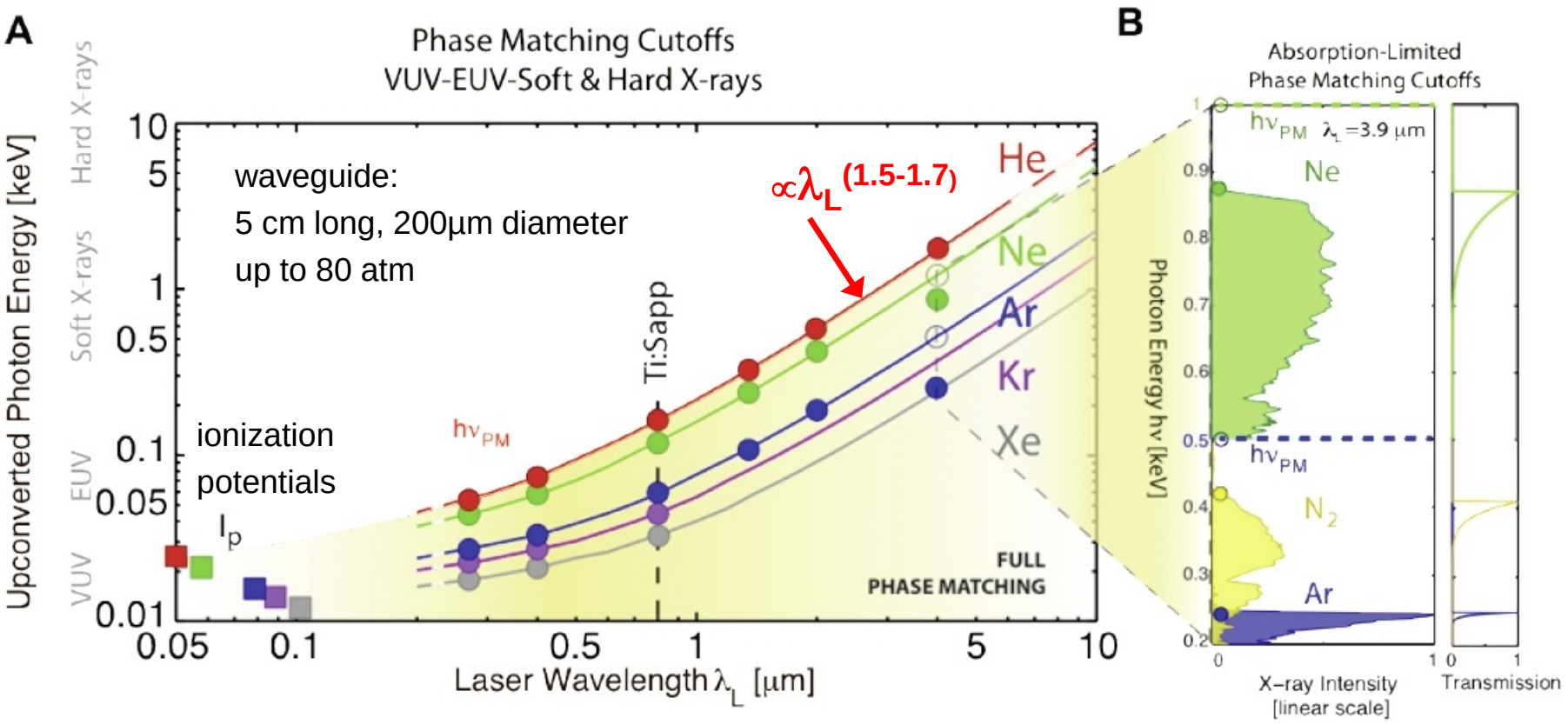

N_2: highest photon energies from molecules
→ dynamic tomographic imaging

observed cutoff for Ar and Ne below predicted cutoff (open circles) due to inner-shell absorption

T. Popmintchev *et al.*, Science **336**, 1287 (2012)

12.3.5 "Perfect wave" synthesis for HHG

synthesized from **800nm + 400nm + 267nm + 200nm + 1600nm**

ω + 2ω + 3ω + 4ω + 0.5 ω

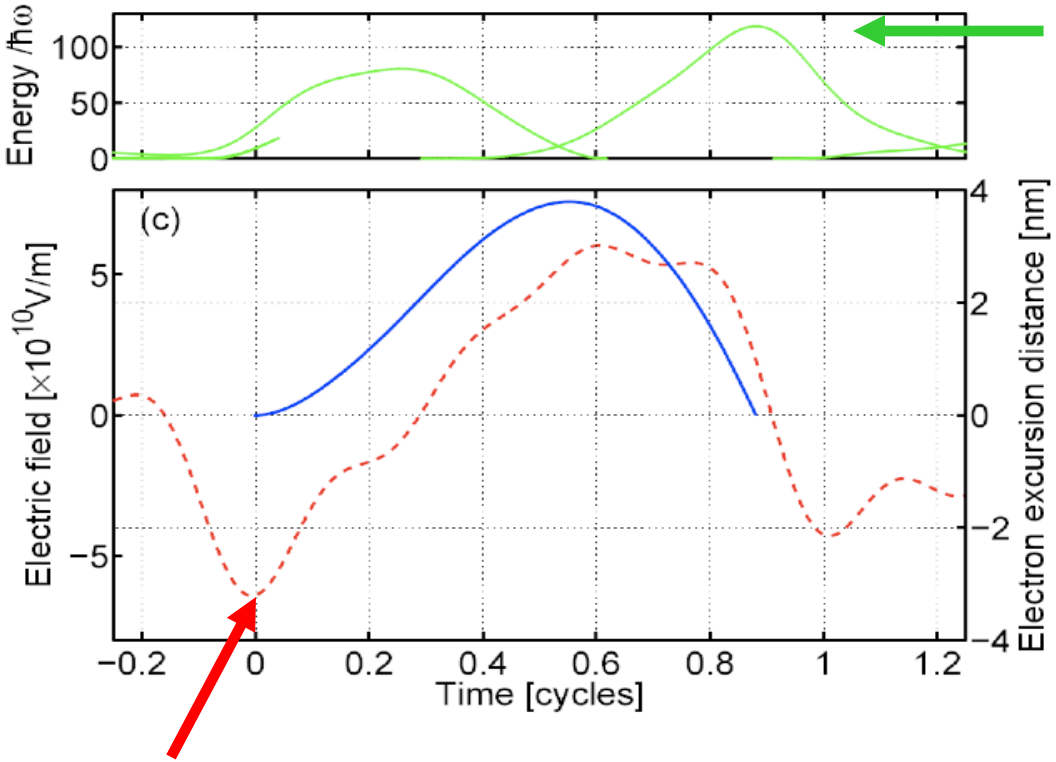

max. recollision energy

waveform	cutoff energy
sinusoidal	~ $3.17U_P$
synthesized	~ $9U_P$

high field here increases ionization probability

L. E. Chipperfield *et al.*, Phys. Rev. Lett. **102**, 063003 (2009)

C. Jin *et al.*, Nature Commun. **5**:4003 (2014)